

Charts to Rapidly Estimate Temperature following Laser Irradiation

Scott A. Prahl

Oregon Medical Laser Center, Portland, OR 97225

ABSTRACT

A recurring problem in laser applications is estimating the thermal response of target tissues to laser irradiation. This typically involves using an optical model to determine the distribution of absorbed laser energy and then using a thermal model to establish the temperature during and after laser irradiation. To avoid such modelling and yet allow one to obtain fast, accurate estimates of temperature, a series of charts for laser irradiation of semi-infinite homogeneous media with adiabatic boundaries is presented. These charts were created using analytic solutions of the temperature for absorbing-only media with simple pulsed source geometries. Through the use of non-dimensional parameters, these charts allow one to make rapid estimates of the spatial and temporal thermal distributions following laser irradiation for arbitrary pulse durations and absorption coefficients.

Keywords: modelling, temperature, scattering, absorbing, thermal confinement, diffusion, chart, graph

1 INTRODUCTION

Many papers have modelled temperatures in tissues following heating. Fewer papers have modelled light distributions in tissue. Still fewer papers have modelled temperatures in tissue following laser irradiation. This is one of those papers.

No general solution to the thermal/optical problem in tissue exists, nor is likely to exist soon, due to the difficulties associated with phase transitions, fracture mechanics, variable optical properties, and tissue inhomogeneities. This paper avoids these difficult problems (and others) by ignoring them. Specifically, I assume (1) a homogeneous material with unchanging optical and thermal properties, (2) semi-infinite geometry, (3) adiabatic thermal boundaries, and (4) no phase-transitions (e.g., no ablation, pyrolysis). The laser irradiation is uniform and perpendicular to the surface and is constant for the duration of the laser pulse. Further, I assume that the diffusion equation is adequate to simulate the light propagation in the turbid medium.

To summarize, the problem solved in this paper is “not too hard” and “not too easy.” Sufficient simplification is made so that analytic solutions can be obtained. Sufficient complexity is retained so that the solutions are interesting and could not be predicted based on length scale arguments alone. For example, the solution remains valid for pulse durations comparable to the thermal diffusion time for the sample. The temperature solution is obtained in closed-form and is valid for at any time or position in the sample. The laser pulse may be an arbitrary length and the sample can have any scattering and absorption coefficients.

2 THEORY

2.1 Optical Distribution

The full radiative transport equation is finessed by assuming that the diffusion approximation is valid. This is not as bad as it might seem. The diffusion approximation is best at approximating integrated quantities like total reflected light. Thus while the diffusion approximation may not get the particulars of the internal distribution of light exactly right, it will get the total absorbed energy nearly correct. Since the specifics of the heating distribution become less important as heat diffuses, and the total energy delivered becomes more important, a combined optical-thermal model plays to the strengths of the optical diffusion approximation.

The diffusion equation in one dimension is¹

$$\frac{d^2 L_d(z)}{dz^2} - \mu_{\text{eff}}^2 L_d(z) = -(3\mu_t^2 - \mu_{\text{eff}}^2)(1 - r_s)E_0 e^{-\mu_t z} \quad (1)$$

where $L_d(z)$ is the total diffuse radiance [W/cm²] at a point, E_0 is the normal irradiance [W/cm²] at the surface, and r_s is the specular reflection at the surface. The total scattering coefficient μ_t [cm⁻¹] and effective attenuation μ_{eff} are

$$\mu_t = \mu_a + \mu_s \quad \text{and} \quad \mu_{\text{eff}} = \sqrt{3\mu_a\mu_t} \quad (2)$$

where μ_a and μ_s are the absorption and scattering coefficients. The scattering phase function is assumed to be isotropic. For anisotropic scattering, the scattering coefficient μ_s should be replaced by the reduced scattering coefficient $\mu_s' = \mu_s(1 - g)$.*

The boundary condition for the top boundary is

$$L_d(z) = \frac{A}{\mu_t} \frac{dL_d(z)}{dz} \quad \text{at} \quad z = 0 \quad \text{and} \quad A = \frac{1 + R_1}{1 - R_1} \quad (3)$$

where R_1 is the normalized first moment of the unpolarized Fresnel reflection.[†] This moment was found analytically by Walsh (see²)

$$\begin{aligned} R_1 = & \frac{1}{2} + \frac{(m-1)(3m+1)}{6(m+1)^2} + \left[\frac{m^2(m^2-1)^2}{(m^2+1)^3} \right] \ln \frac{m-1}{m+1} \\ & - \frac{2m^3(m^2+2m-1)}{(m^2+1)(m^4-1)} + \left[\frac{8m^4(m^4+1)}{(m^2+1)(m^4-1)^2} \right] \ln m \end{aligned} \quad (4)$$

where $m = 1/n$ is the reciprocal of the index of refraction of the slab (relative to the medium above the slab). The second boundary condition requires

$$L_d(z) \rightarrow 0 \quad \text{as} \quad z \rightarrow \infty$$

The total radiance in the slab is the sum of the scattered and unscattered radiances

$$L(z) = L_d(z) + (1 - r_s)E_0 \exp(-\mu_t z)$$

Therefore

$$L(z) = \frac{1}{3a - 2} \left[\frac{3a(3 + 2A)}{3 + 2A\sqrt{3 - 3a}} \exp(-\mu_{\text{eff}} z) - 2 \exp(-\mu_t z) \right] (1 - r_s)E_0 \quad (5)$$

*This approximation replaces the phase function by a delta-isotropic phase function. This is not as accurate as a delta-Eddington phase function, but can be easily incorporated into this derivation. I did not include the anisotropy in an effort to eliminate yet another variable in the derivation.

[†]Technically, $A = (1 + R_1)/(1 - R_2)$ where R_2 is the normalized second moment of the Fresnel reflection. Ironically, R_1 gives better approximations when used in the denominator than R_2 and therefore R_2 is not used.

where the single scattering albedo a is defined as

$$a = \frac{\mu_s}{\mu_a + \mu_s}$$

The normalized volumetric heat generation in the tissue is

$$q'''(z) = \mu_a(1 - r_s)E_0 \left\{ \left[\frac{3a}{3a - 2} \frac{3 + 2A}{3 + 2A\sqrt{3 - 3a}} \right] \exp(-\mu_{\text{eff}}z) + \left[\frac{2}{2 - 3a} \right] \exp(-\mu_t z) \right\} \quad (6)$$

2.2 Thermal Evolution

The one-dimensional heat conduction equation is

$$\frac{\partial^2 T}{\partial z^2} = \frac{1}{\kappa} \frac{\partial T}{\partial t} \quad (7)$$

where T is the temperature, t is time, and κ is the thermal diffusivity. The Green's function for an instantaneous plane source (triggered at t') in an infinite uniform medium is³

$$G(z, t; z', t') = \frac{1}{\sqrt{4\pi\kappa(t - t')}} \exp \left[-\frac{(z - z')^2}{4\kappa(t - t')} \right] \quad (8)$$

Note that the Green's function has the somewhat peculiar dimensions of [1/cm]. The temperature for an arbitrary volumetric heating distribution $\mu_a L(z', t')$ is

$$T(z, t) = \frac{\mu_a}{\rho c} \int_0^\infty \int_0^{t_p} G(z, t; z', t') L(z', t') dz' dt' \quad (9)$$

where ρc is the specific heat of the material.

The Green's function a pulsed plane source that is constant and lasts from $t' = 0$ to $t' = t_p$ is

$$G(z, t; z') = \frac{1}{t_p} \int_0^{t_p} G(z, t; z', t') dt' \quad (10)$$

Substituting and integrating yields

$$\begin{aligned} G(z, t; z') &= \sqrt{\frac{t}{\pi t_p^2 \kappa}} \exp \left[-\frac{(z - z')^2}{4\kappa t} \right] + \frac{z - z'}{2\kappa t_p} \operatorname{erf} \left[\frac{z - z'}{\sqrt{4\kappa t}} \right] \\ &- \sqrt{\frac{t - t_p}{\pi t_p^2 \kappa}} \exp \left[-\frac{(z - z')^2}{4\kappa(t - t_p)} \right] - \frac{z - z'}{2\kappa t_p} \operatorname{erf} \left[\frac{z - z'}{\sqrt{4\kappa(t - t_p)}} \right] \end{aligned}$$

This solution is valid even when ($0 \leq z \leq z'$) if one recalls that $-\operatorname{erf}(z) = \operatorname{erf}(-z)$. One might note that this solution is identical to equation 2-185 in Özisik who obtained the solution when $t = t_p$.⁴

The Green's function in a semi-infinite medium with no heat flow across the boundary $z = 0$ is obtained by the method of images as

$$G_{\text{adiabatic}}(z, t; z', t') = \frac{1}{\sqrt{4\pi\kappa(t - t')}} \left(\exp \left[-\frac{(z - z')^2}{4\kappa(t - t')} \right] + \exp \left[-\frac{(z + z')^2}{4\kappa(t - t')} \right] \right) \quad (11)$$

and therefore the Green's function for a pulsed source in a semi-infinite material with adiabatic boundaries is

$$G_{\text{adiabatic}}(z, t; z') = G(z, t; z') + G(z, t; -z') \quad (12)$$

2.3 Optical-thermal solution

Since the normalized volumetric heat generation in the sample contains decaying exponential factors, here the temperature response for a simple exponential is useful,

$$G(z, t) = \int_0^\infty G(z, t; z') \exp(-\mu_t z') dz' \quad (13)$$

The parameter μ_t introduces a convenient length scale with which to form dimensionless variables. For example,

$$\xi = \mu_t z \quad \text{and} \quad \tau = \mu_t^2 \kappa t \quad (14)$$

At this point we also note that the Green's function $G(\xi, \tau)$ is dimensionless,

$$G(\xi, \tau) = \int_0^\infty G(\xi, \tau; \xi') \exp(-\xi') d\xi' \quad (15)$$

Substituting and integrating by parts yields[‡]

$$\begin{aligned} G(\xi, \tau) = & \frac{1}{2\tau_p} \left\{ 4\sqrt{\frac{\tau}{\pi}} \exp\left[-\frac{\xi^2}{4\tau}\right] - 4\sqrt{\frac{\tau - \tau_p}{\pi}} \exp\left[-\frac{\xi^2}{4(\tau - \tau_p)}\right] + 2\xi \operatorname{erf}\left[\frac{\xi}{2\sqrt{\tau}}\right] - 2\xi \operatorname{erf}\left[\frac{\xi}{2\sqrt{\tau - \tau_p}}\right] \right. \\ & + \exp(\tau - \xi) \operatorname{erfc}\left[\sqrt{\tau} - \frac{\xi}{2\sqrt{\tau}}\right] - \exp(\tau - \tau_p - \xi) \operatorname{erfc}\left[\sqrt{\tau - \tau_p} - \frac{\xi}{2\sqrt{\tau - \tau_p}}\right] \\ & \left. + \exp(\tau + \xi) \operatorname{erfc}\left[\sqrt{\tau} + \frac{\xi}{2\sqrt{\tau}}\right] - \exp(\tau - \tau_p + \xi) \operatorname{erfc}\left[\sqrt{\tau - \tau_p} + \frac{\xi}{2\sqrt{\tau - \tau_p}}\right] \right\} \end{aligned}$$

A useful special case is the temperature at the surface $\xi = 0$

$$G(0, \tau) = \frac{1}{\tau_p} \left\{ 2\sqrt{\frac{\tau}{\pi}} - 2\sqrt{\frac{\tau - \tau_p}{\pi}} + \exp(-\tau) \operatorname{erfc}(\sqrt{\tau}) - \exp(-\tau_p + \tau) \operatorname{erfc}(\sqrt{\tau - \tau_p}) \right\} \quad (16)$$

The temperature during the laser pulse ($\tau \leq \tau_p$) is[§]

$$\begin{aligned} G(\xi, \tau) = & \frac{1}{2\tau_p} \left\{ 4\sqrt{\frac{\tau}{\pi}} \exp\left[-\frac{\xi^2}{4\tau}\right] - 2\xi \operatorname{erfc}\left[\frac{\xi}{2\sqrt{\tau}}\right] - 2\exp(-\xi) \right. \\ & \left. + \exp(\tau - \xi) \operatorname{erfc}\left[\sqrt{\tau} - \frac{\xi}{2\sqrt{\tau}}\right] + \exp(\tau + \xi) \operatorname{erfc}\left[\sqrt{\tau} + \frac{\xi}{2\sqrt{\tau}}\right] \right\} \end{aligned}$$

The surface temperature during the laser pulse is,

$$G(0, \tau) = \frac{1}{\tau} \left\{ 2\sqrt{\frac{\tau}{\pi}} + \exp(-\tau) \operatorname{erfc}(\sqrt{\tau}) - 1 \right\} \quad (17)$$

The limiting behavior for small times should lead to a function that is proportional to unity

$$G(0, \tau) = 1 - \frac{4}{3\sqrt{\pi}} \sqrt{\tau} + \frac{1}{2} \tau - \dots \quad (18)$$

The temperature in the sample at an arbitrary time and position and for any pulse duration, absorption coefficient, or anisotropy is then

$$T(z, t) = \frac{\mu_a(1 - r_s)E_0 t_p}{\rho c(3a - 2)} \left[\frac{3a(3 + 2A)}{3 + 2A\sqrt{3} - 3a} G(\mu_{\text{eff}} z, \mu_{\text{eff}}^2 \kappa t) - 2G(\mu_t z, \mu_t^2 \kappa t) \right] \quad (19)$$

[‡]A simple check of the validity of this expression is to integrate over all space. The result should be and was unity

[§]I have normalized by the time τ instead of by τ_p because all the energy has not been delivered.

In the special case of an absorbing only material, the temperature is

$$T(z, t) = \frac{(1 - r_s)\mu_a E_0 t_p}{\rho c} G(\mu_a z, \mu_a^2 \kappa t) \quad (20)$$

This suggests the following form for the dimensionless temperature

$$\Theta(z, t) = \frac{\rho c T(z, t)}{\mu_a (1 - r_s) E_0 t_p} = \frac{1}{3a - 2} \left[\frac{3a(3 + 2A)}{3 + 2A\sqrt{3 - 3a}} G(\mu_{\text{eff}} z, \mu_{\text{eff}}^2 \kappa t) - 2G(\mu_t z, \mu_t^2 \kappa t) \right] \quad (21)$$

The dimensionless temperature Θ is therefore normalized to the temperatures that would arise if there were no optical or thermal diffusion. The temperature $\Theta = 1$ corresponds to the temperature distribution associated with an infinitely short pulse on an absorbing-only target.

3 DISCUSSION

Figures 1–8 graph the dimensionless temperature against a variety of parameters. The captions provide a brief interpretation of the charts.

I believe that this paper presents the first closed-form solution to the one-dimensional, pulsed, optical-thermal problem incorporating scattering and absorption. This solution is sufficiently simple that it can be coded in a few lines of one of the current computer algebra systems (*Maple* or *Mathematica*). The solution should aid in making informed estimates of the implications of changing laser wavelength (and therefore absorption coefficient) or of changing the laser pulse characteristics. This is especially helpful when the time for thermal relaxation (across dimensions comparable to the optical mean free path) is approximately equal to the duration of the laser pulse. Finally, because this solution is exact it can also provide a useful check for more elaborate optical-thermal numerical simulations.

4 REFERENCES

- [1] A. Ishimaru, *Wave Propagation and Scattering in Random Media*, vol. 1. New York: Academic Press, 1978.
- [2] J. W. Ryde, “The scattering of light by turbid media—Part I,” *Proc. Roy. Soc. (London)*, vol. A131, pp. 451–464, 1931.
- [3] H. S. Carslaw and J. C. Jaeger, *Conduction of Heat in Solids*. Oxford: Clarendon Press, second ed., 1986.
- [4] M. N. Özışık, *Boundary Value Problems of Heat Conduction*. New York: Dover, 1968.

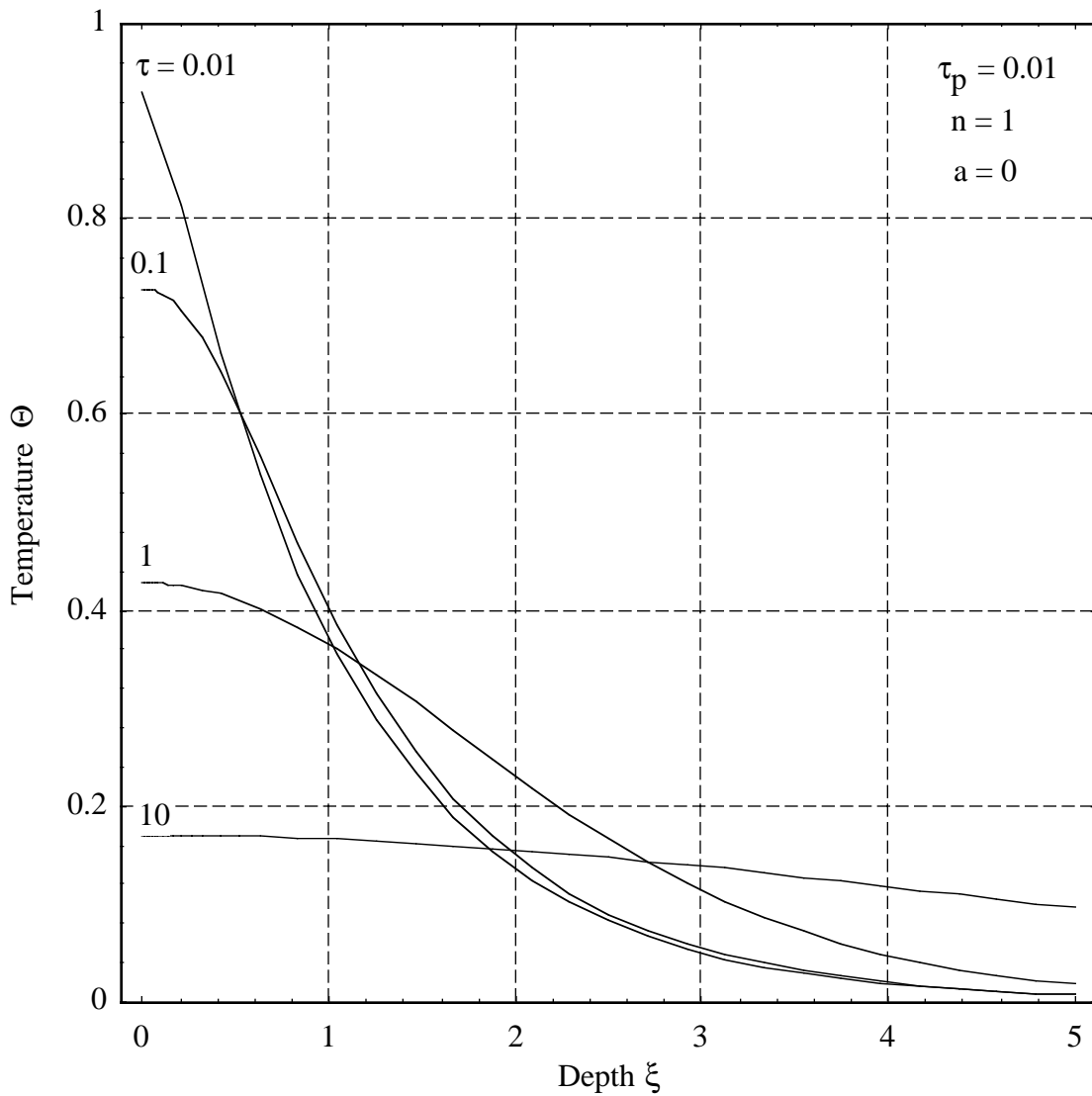


Figure 1: The thermal evolution of a very short pulse ($\tau_p = 0.01$). Even for such a short pulse, the surface temperature only reaches about 95% of the temperature increase expected for an infinitely short pulse. The decrease in temperature between the end of the laser pulse at $\tau = 0.01$ and $\tau = 0.1$ is roughly equal to the decay between $\tau = 0.1$ and $\tau = 1$, or between $\tau = 1$ and $\tau = 10$.

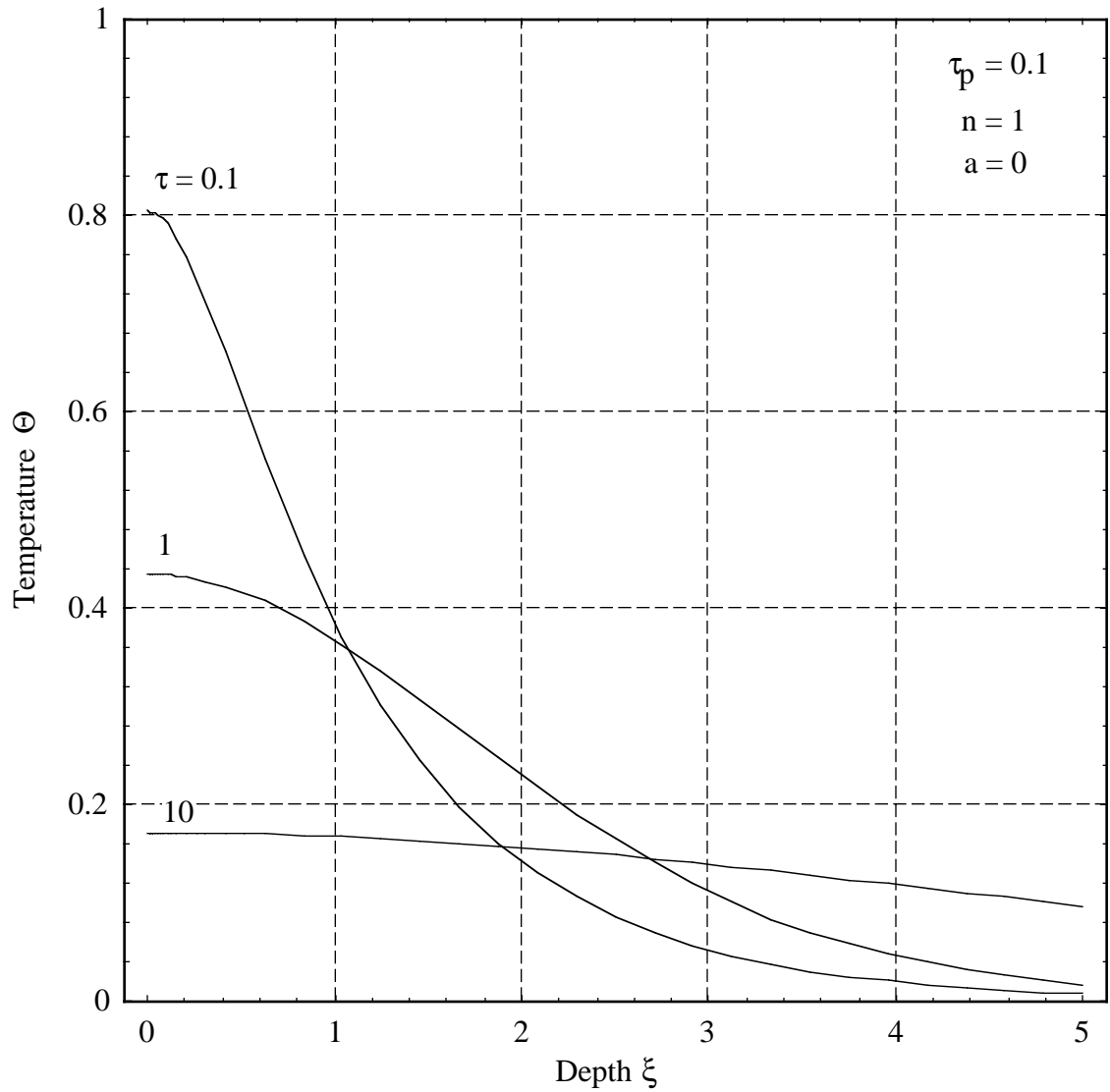


Figure 2: The thermal evolution of a short pulse ($\tau_p = 0.1$). The surface temperature at ($\tau = 0.1$) is greater than that for the very short pulse ($\tau = 0.01$) at the same time, because of the larger temperature gradients associated with the very short pulse. By $\tau = 1$ the internal temperature fields are nearly identical.

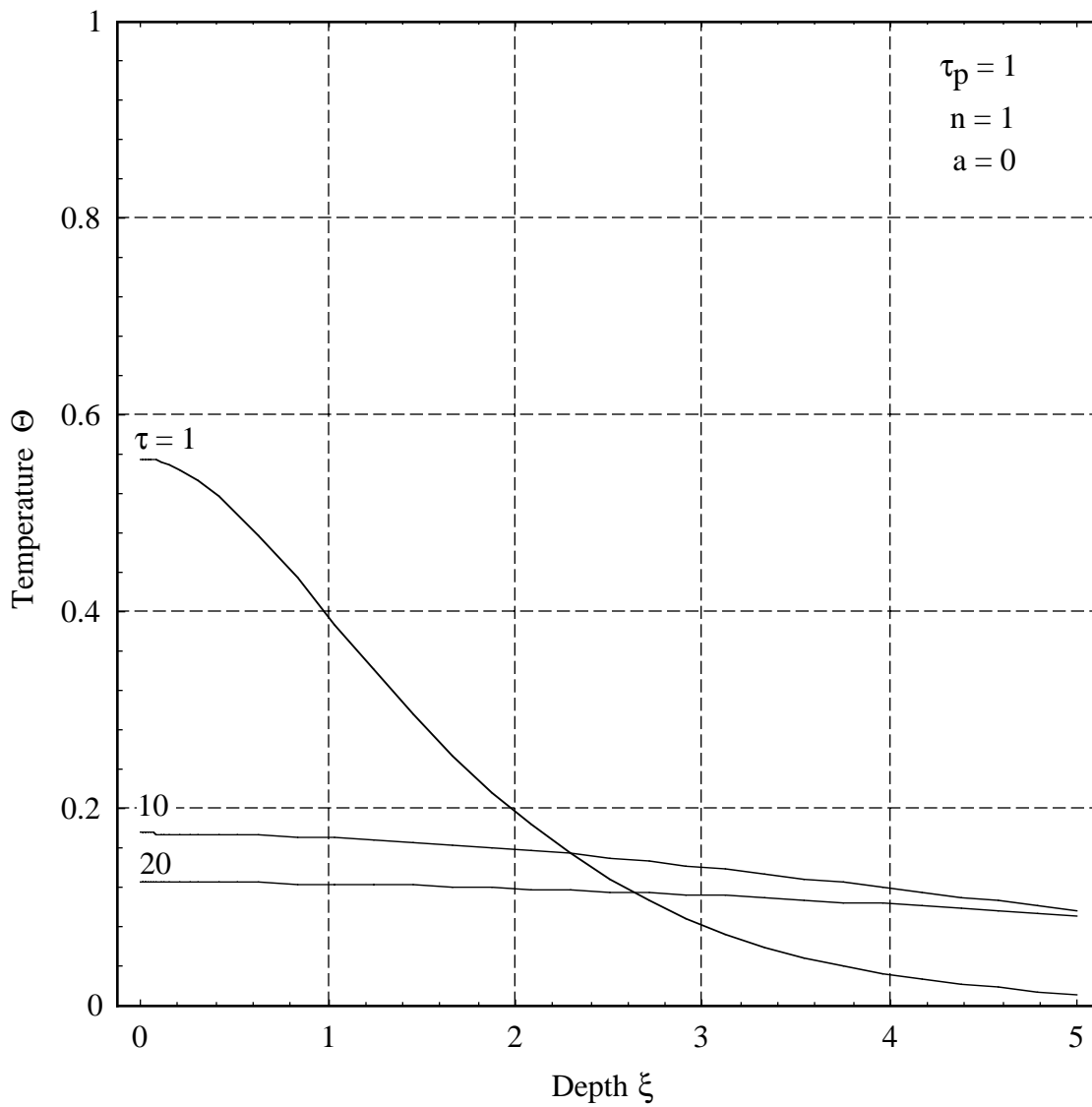


Figure 3: The thermal evolution of a medium length pulse ($\tau_p = 1$). The surface temperature at $\tau = 1$ is much higher than for the shorter pulses at the same time. Again, by $\tau = 10$ internal temperature fields are nearly identical for all three pulse lengths.

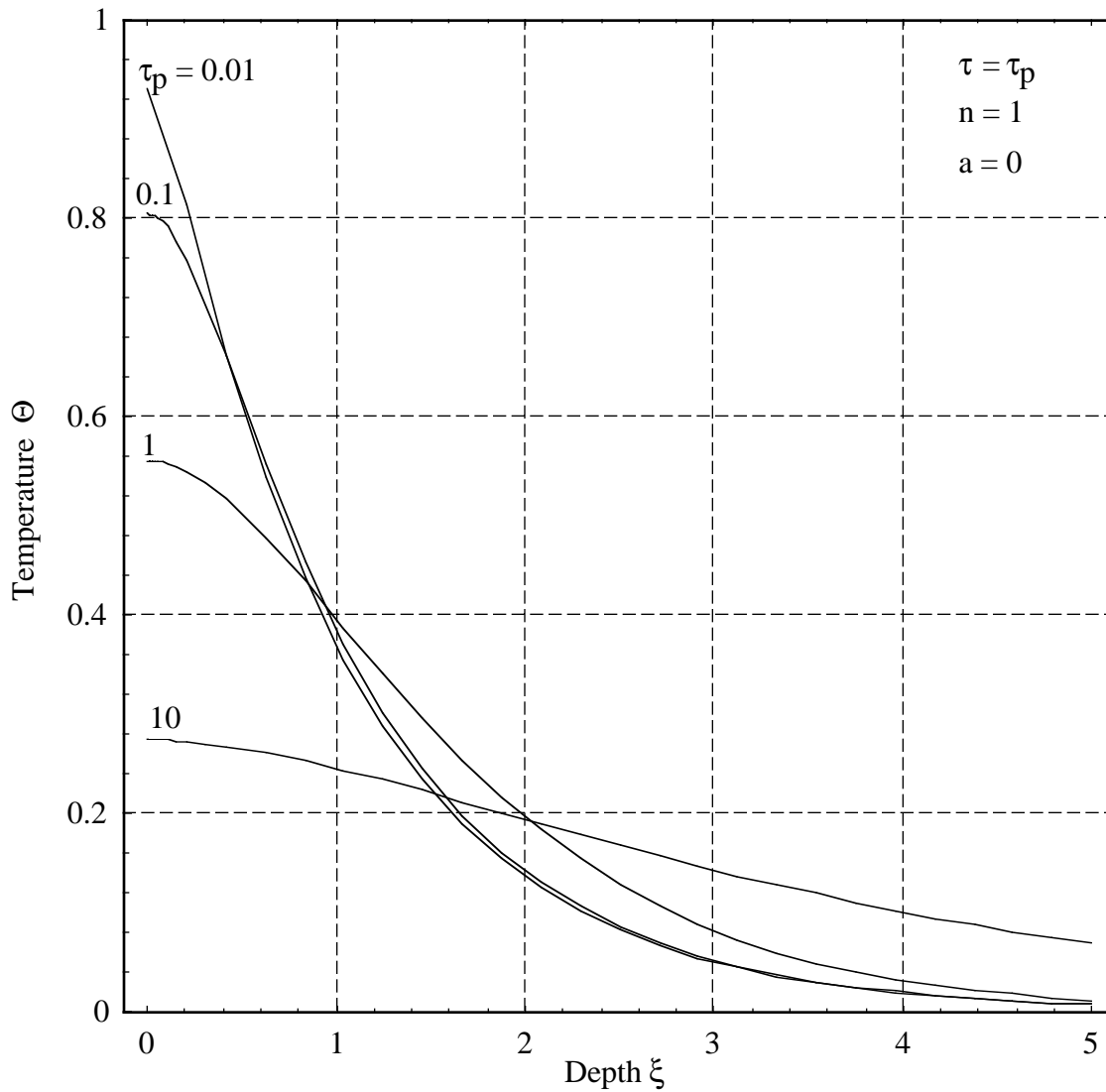


Figure 4: The internal spatial distribution is displayed at the end of the laser pulse to demonstrate thermal confinement. These times correspond to the maximum surface temperatures for the four different pulse lengths. Clearly, the two shortest pulse lengths achieve the nearly same degree of thermal confinement. When the pulse duration is equal to unity, the thermal penetration is significantly deeper than for the shorter pulses.

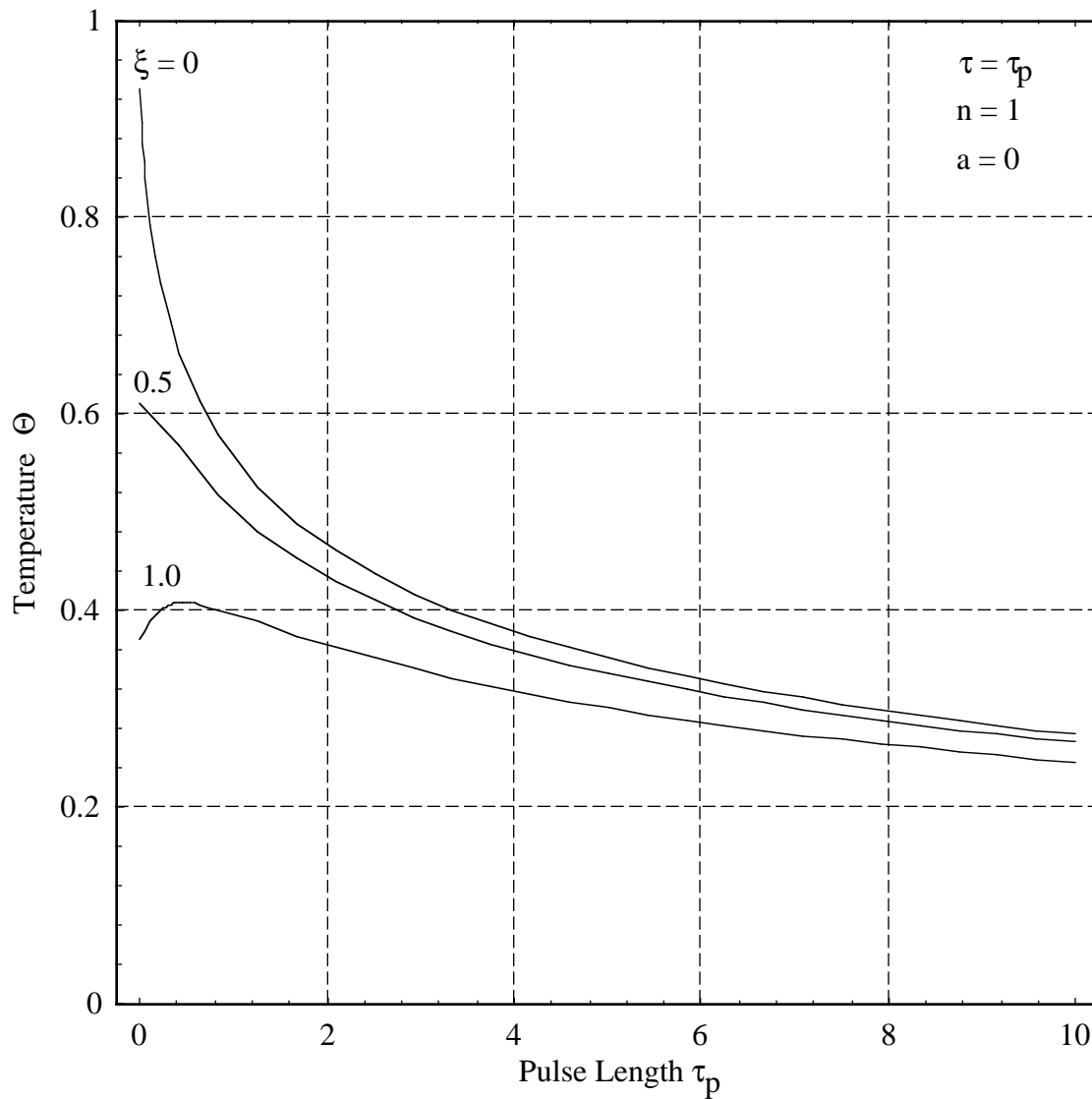


Figure 5: The effect of pulse length on surface temperature. For very short pulse lengths ($\tau_p \rightarrow 0$) the surface temperature approaches unity as expected. Since the temperature is plotted at the end of the pulse, the surface temperatures are the maximum temperatures achieved in the tissue. Consequently, this graph is handy for estimating how long a laser pulse must be to ensure that the tissue temperature stays below a fixed temperature. The other two lines $\xi = 0.5$ and $\xi = 1$ indicate how uniform the internal temperature profile is at the end of the laser pulse.

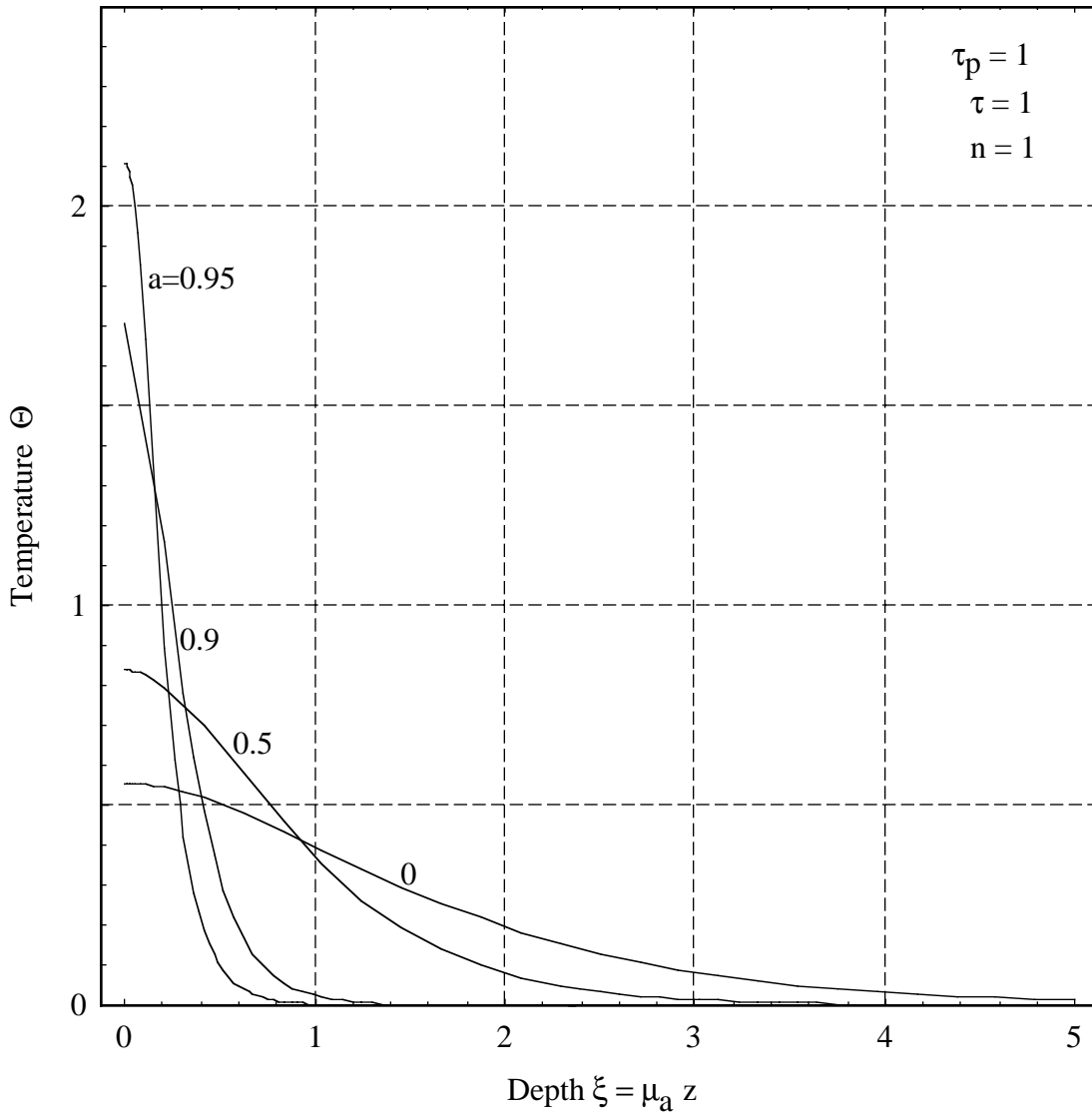


Figure 6: The effect of scattering on temperature. The dimensionless depth and time are specified in terms of the dimensionless variables $\xi = \mu_a z$ and $\tau = \mu_a^2 \kappa t$. The best way to interpret this graph is to assume that the absorption coefficient remains fixed. Increased albedo implies increased scattering coefficient. Adding scattering to the sample improves the thermal confinement and longer pulse lengths may be used to achieve the same degree of thermal confinement.

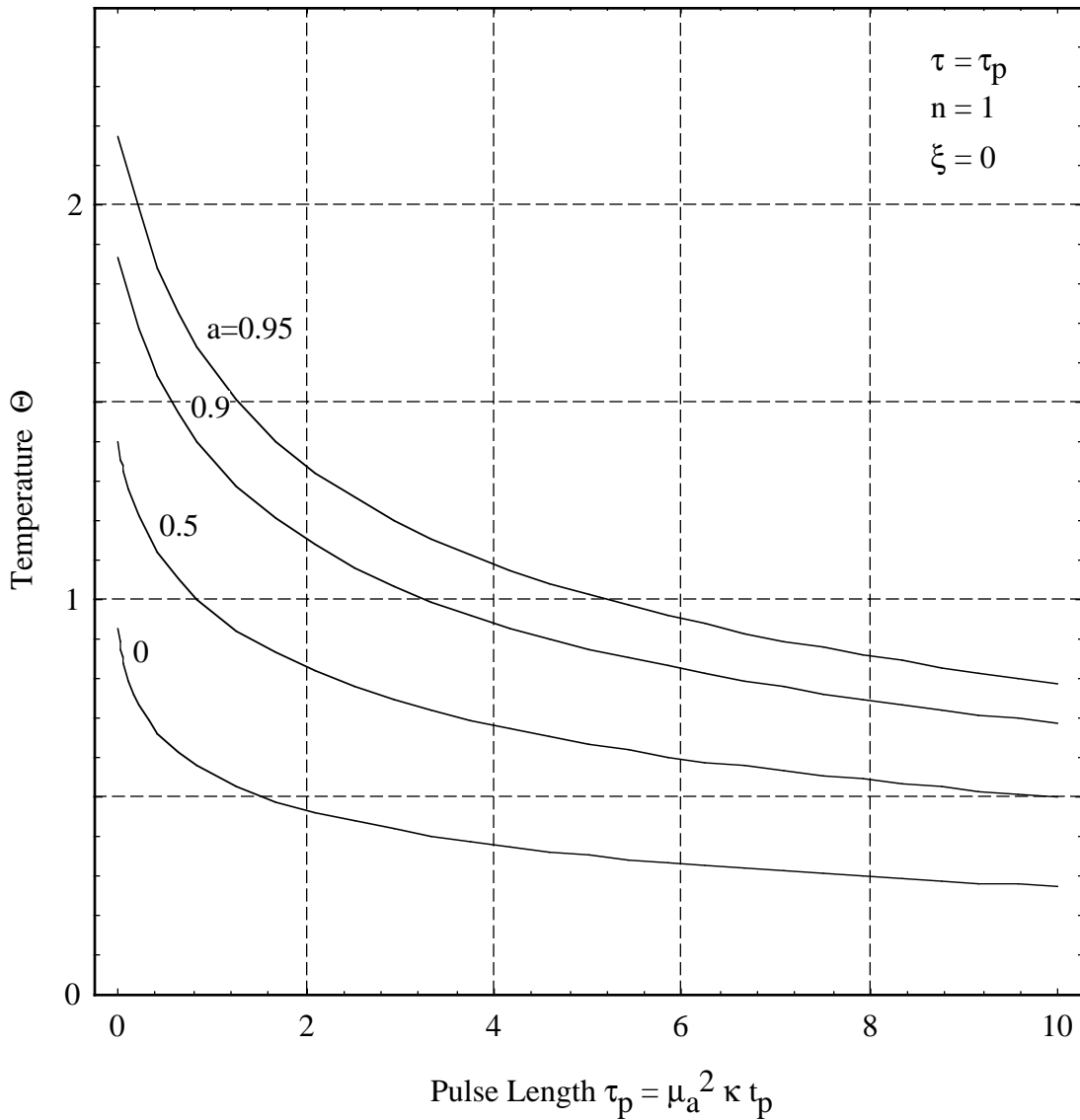


Figure 7: The effect of scattering on surface temperature. The best way to interpret this graph is assume that the absorption coefficient remains fixed. The dimensionless time is specified in terms of $\tau = \mu_a^2 \kappa t$. Increasing the scattering coefficient and hence the albedo increases the surface temperature, because the light does not penetrate as deeply. Note that light must be deposited much more slowly in highly scattering tissues than in absorbing-only tissues to ensure that the tissue is not heated too much.

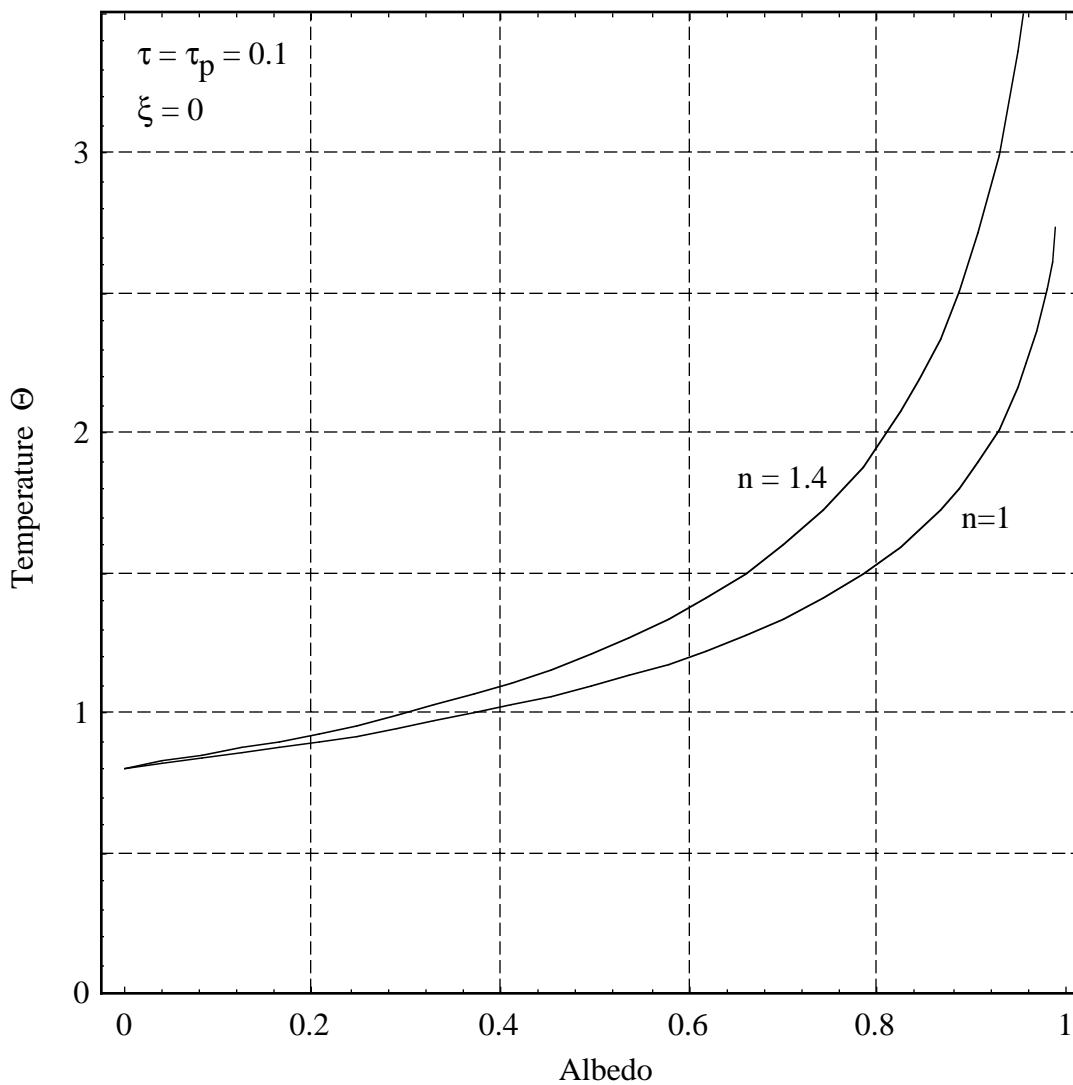


Figure 8: The surface temperatures for matched and mismatched boundaries for a short laser pulse. Increasing the index of refraction mismatch increases the subsurface fluence distribution and leads to increased surface temperatures. Note that for mismatched boundaries it only takes $\mu_s \approx 4\mu_a$ to achieve twice the absorbing-only surface temperature, but for matched boundaries $\mu_s \approx 10\mu_a$ is required.